Available online at www.sciencedirect.com
SCIENCE DIRECT®
Chemical Physics 298 (2004) 279–297
Chemical Physics
www.elsevier.com/locate/chemphys

Photoion mass spectrometry of five amino acids in the 6–22 eV photon energy range

Hans-Werner Jochims [a], Martin Schwell [b], Jean-Louis Chotin [b], Monique Clemino [b], François Dulieu [b,c], Helmut Baumgärtel [a], Sydney Leach [b,c,*]

[a] *Institut für Physikalische und Theoretische Chemie der Freien Universität Berlin, Takustr. 3, 14195 Berlin, Germany*
[b] *Laboratoire d'Etude du Rayonnement et de la Matière en Astrophysique (LERMA), CNRS-UMR 8112, Observatoire de Paris-Meudon, 5 place Jules-Janssen, 92195 Meudon, France*
[c] *LAMAP, Département de Physique, Université Cergy-Pontoise, 95031 Cergy Pontoise Cedex, France*

Received 16 June 2003; accepted 28 November 2003

Abstract

A photoionization mass spectrometry study in the 6–22 eV photon energy region of five amino acids, glycine-h_5 and its -d_5 isotopologue, α-alanine, β-alanine, α-aminoisobutyric acid and α-valine, revealed VUV-induced degradation pathways of these important biological molecules. The fragmentation patterns, ionization energies and ion appearance energies are reported, many for the first time, and are compared with results of electron impact and other studies. Assignment of ion peaks and determination of fragment ion formation channels were assisted by mass spectral data on deuterated isotopologues of the three proteinaceous amino acids studied. Thermochemical data, coupled with the observed ion appearance energies, was also useful in clarifying dissociative photoionization pathways. Ion pair formation appears to occur in certain low energy dissociation processes. Isomeric interconversion between α-alanine and β-alanine cations does not occur up to 20 eV excitation energy. Some astrophysical implications concerning the prospects for amino acid observation and survival in the interstellar medium and in meteorites are briefly discussed.

1. Introduction

The vacuum ultraviolet (VUV) photophysics and photochemistry of amino acids is of considerable interest in view of the possible delivery of these molecules, and even more complex molecular species, from space to the primitive Earth, and the role that they could have played in the origin and development of life on our planet [1]. Amino acids are found in both meteorites and micrometeorites [2,3] and much effort is currently being undertaken to observe them in the interstellar medium (ISM) [4]. Since this work was submitted for publication, the simplest amino acid, glycine, has been reported to have been observed by radioastronomy in hot molecular cores in three regions of ongoing massive star formation, and it was suggested that other amino acids could be formed in these or similar sites [5]. The physical conditions in these regions of the ISM are those which are suggested by our results as propitious for observation of interstellar amino acids. This confirms our proposition that knowledge of the photostability of amino acids in the VUV is important for assessing which spatial regions are likely sources for observation of interstellar amino acids and/or their degradation products. This interest extends to laboratory simulations of amino acid production in comets under UV irradiation [6,7]. We remark that detailed knowledge of photodegradation processes is particularly important in the VUV since photoionization and dissociative ionization can become very efficient in this photon energy region [8].

In this paper, we report results of a photoionization mass spectrometry (PIMS) study of five amino acids: glycine (h_5 and d_5), α-alanine, β-alanine, α-aminoisobutyric acid and α-valine. Three of these amino acids, glycine, α-alanine and α-valine, are proteinaceous, while all five have been found in meteoritic materials [3]. We

* Corresponding author. Address: Laboratoire d'Etude du Rayonnement et de la Matière en Astrophysique (LERMA), CNRS-UMR 8112, Observatoire de Paris-Meudon, 5 place Jules-Janssen, 92195 Meudon, France. Tel.: +33-1-4507-7561; fax: +33-1-4507-7100.
E-mail address: sydney.leach@obspm.fr (S. Leach).

0301-0104/$ - see front matter © 2003 Elsevier B.V. All rights reserved.
doi:10.1016/j.chemphys.2003.11.035

remark that in solution, and in particular in biological media, amino acids exist as zwitterions over a considerable range of pH values, but that in the gas phase, as in our experiments, it is the non-zwitterionic form that is the most stable. In fact, there is at present no experimental or theoretical evidence for a gas phase zwitterion ground state of any amino acid [9,10]. Gas phase studies of amino acids are thus of significance in biology for understanding and determining properties of these basic units free from interactions and, as mentioned above, they are important in several areas of astrophysics.

The photoion yield curves of the amino acid parent and fragment ions were measured as a function of incident photon energy in the 6–22 eV range. We report ionization energy (IE) and fragment appearance energies (AE) that were previously unknown. The photoion fragmentation patterns at an incident energy of 10 or 20 eV are compared with the ion fragmentation patterns obtained by 70 eV electron impact ionization processes. Assignment of the mass spectra of the three proteinaceous α-amino acids glycine, α-alanine and α-valine was aided by 70 eV electron impact mass spectral data on their -d_3 isotopologues, in which the carboxyl and amino hydrogens of the hydrogenated amino acids have been replaced by deuterium atoms [11].

The photoabsorption cross section of the amino acids studied is much higher in the VUV as compared with the UV [12,13]. In particular, all of these molecules absorb strongly at 10.2 eV, where the Lyman-α stellar emission is intense. Furthermore, in connection with the possible Earthbound delivery of biotic molecules from space, we note that the VUV luminosity of the early sun, during the Hadean period of considerable bombardment of the Earth from space, was about two orders of magnitude higher than it is today, although the total luminosity was less [14].

Preliminary accounts of this work have been reported elsewhere, in an exobiology context [15,16]. More detailed implications of the astrophysical and exobiological implications of our results will be reported elsewhere [17].

2. Experimental

Synchrotron radiation from the Berlin electron storage ring BESSY I was monochromatised by a 1.5 m Au grating monochromator (modified McPherson) and then focussed into a differentially pumped gas cell which can be heated up to 400 °C but was here restricted to lower temperatures. The experimental set-up is described in more detail elsewhere [18]. The amino acid vapours were introduced into the ionization chamber by direct evaporation of solid samples in open containers placed 1–2 cm below the position of the incident VUV radiation within the ion extraction zone. The whole chamber was heated to temperatures, typically 150–200 °C, which provided an adequate stream of target molecules but were sufficiently low to ensure that the thermally fragile low volatile amino acids remained undissociated in the gas phase. When some thermally induced dissociation did occur this was easily identified by the observed mass spectra, thus enabling us to modify experimental parameters so as to achieve satisfactory experimental conditions of minimal thermal dissociation. In cases where water impurity was observed in the mass spectra this generally resulted from residues of cleaning procedures of the apparatus which were carried out between experimental runs.

Parent and fragment ions formed by photoionization of the amino acids were measured using a quadrupole mass spectrometer (Leybold Q200), and ion yield curves were obtained through photon energy scans with measuring intervals of 0.025 eV. The yield curves of the principal ions observed are presented in the appropriate figures. Transmitted photons were detected by the fluorescence of a sodium salicylate coated window. Spectral bandwidth of the incident monochromatic radiation was typically 2 Å. Some experiments were carried out with a LiF filter (cut-off effective at 11.4 eV) in order to suppress stray light and second-order radiation. Ion appearance energies were determined mainly with the aid of semi-log plots of the ion yield curves. The amino acid samples were commercial products (Sigma-Aldrich) of best available purity. The formulae of the five amino acids studied are given in Fig. 1.

3. Results and discussion

3.1. Glycine NH_2CH_2COOH (elemental composition: $C_2H_5NO_2$)

The mass spectrum of glycine-h_5 obtained at a photon energy of 10 eV (124 nm) and the corresponding spectrum of glycine-d_5 at a photon energy of 20 eV (62 nm) are given in Fig. 2 and the intensities and values of the m/z peaks are reported in Table 1. For glycine-h_5, apart from the $m/z = 76$ peak, due to protonated glycine, only three ions were detected at 10 eV excitation, at $m/z = 75$, 30 and 28. These are also the principal peaks in 70 eV electron impact mass spectra, which contain 10 features. The glycine-d_5 mass spectrum at 20 eV photon energy also exhibits 10 ion peaks, as well as a deuteronated glycine-d_5 peak at $m/z = 82$. The three different electron impact results for glycine-h_5 given in Table 1 are from three sources, respectively Junk and Svec [11], CRC Spectrochemical Atlas [19] and NIST [20]. Differences in their respective relative ion yields are small but illustrate the sensitivity of such measurements to instrumental and procedural factors.

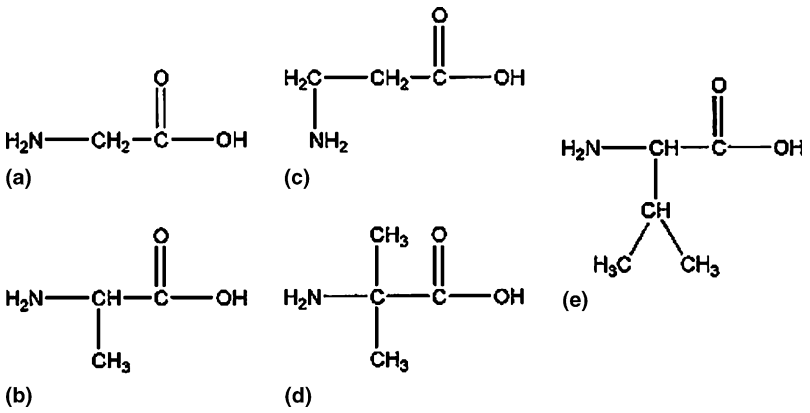

Fig. 1. Five amino acids investigated in the present study: (a) glycine; (b) α-alanine; (c) β-alanine; (d) α-aminoisobutyric acid; (e) α-valine.

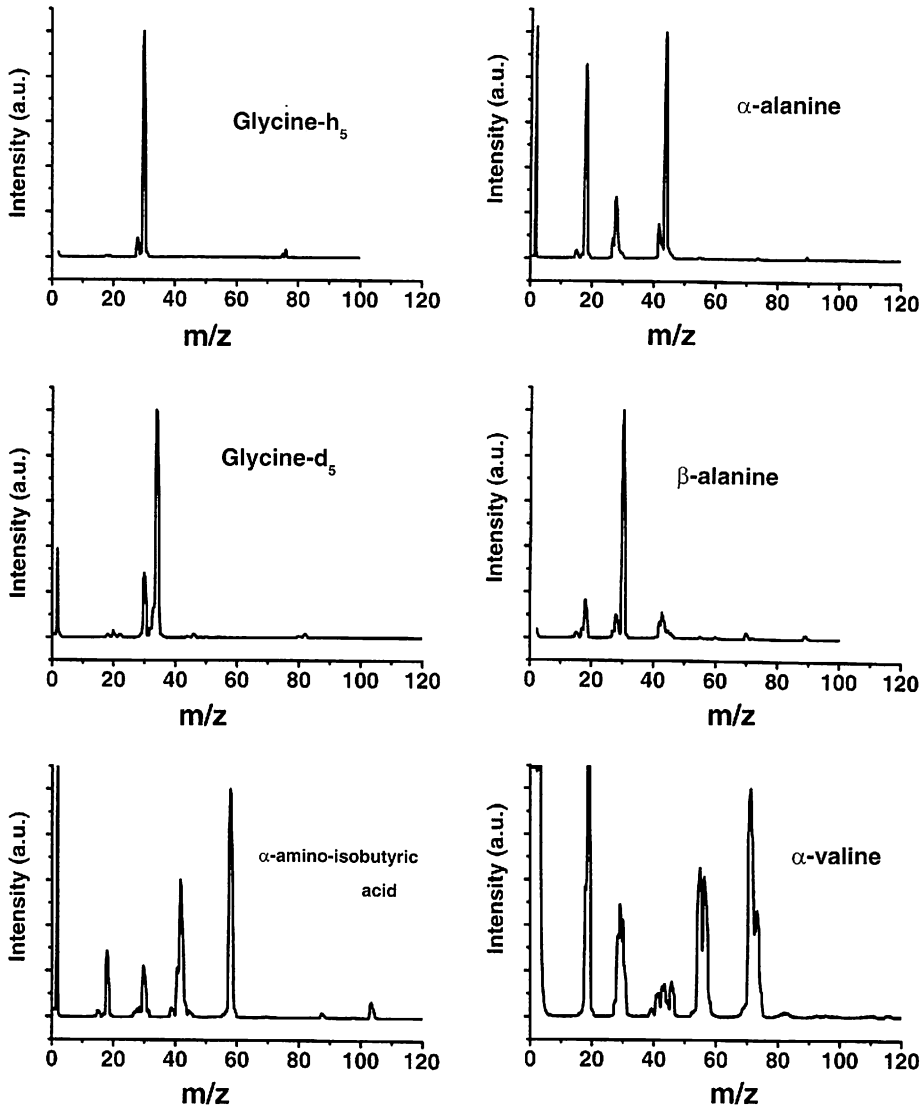

Fig. 2. Photoion mass spectra of glycine-h_5, glycine-d_5, α-alanine, β-alanine, α-aminoisobutyric acid and α-valine. Photon excitation energy 20 eV except for glycine-h_5 (10 eV).

Table 1
Glycine-h_5 NH_2CH_2COOH and glycine-d_5 ND_2CD_2COOD

m/z gly-h_5	Gly-h_5 electron impact 70 eV relative intensity[a]	Gly-h_5 photon impact 10 eV relative intensity	Gly-h_5 photon impact AE/eV	Ion assignments glycine-h_5	m/z gly-d_5	Gly-d_5 photon impact 20 eV relative intensity	Gly-d_5 photon impact AE/eV	Ion assignments glycine-d_5
75	6 (6) *5*	3	9.02 ± 0.02	$NH_2CH_2COOH^+$	80	2	9.07 ± 0.03	$ND_2CD_2COOD^+$
45	3 (3) *3*	0		$HOCO^+$	46	2		$DOCO^+$
44	3 (3) *3*	0		CO_2^+	44	1		CO_2^+
31	2 (2) *0*	2		$NH_2{}^{13}CH_2^+$ $NH_2CH_3^+$	36	1		$ND_2CD_3^+$
30	100	100	9.38 ± 0.05	$NH_2CH_2^+$	35	2		$ND_2{}^{13}CD_2^+$
29	1 (1) *4*	0		NH_2CH^+	34	100	9.50 ± 0.05	$ND_2CD_2^+$
28	21 (21) *25*	9	$13.0^b \pm 0.1$	$HCNH^+$	33	12		Isotopic impurity ND_2CHD^+; $NHDCD_2^+$
27	2 (2) *3*	0		$C_2H_3^+$	32	4		ND_2CD^+
18	1 (1) *N/A*	1		NH_4^+	30	27	$13.1^b \pm 0.1$	$DCND^+$
					22	1	13.4 ± 0.1	ND_4^+
					20	2		ND_3^+
					18	1		ND_2^+

Mass spectra and appearance energies (AE). Ion assignments of m/z peaks.

[a] The three successive values of each mass peak relative intensity are from Junk and Svec [11], in brackets from the NIST collection [20], in italics from the CRC compilation [19].

[b] This ion yield curve also has a low energy tail, see text.

3.1.1. The parent ion $NH_2CH_2COOH^+$: $m/z = 75$

The weakness of the $m/z = 75$ signal in the glycine-h_5 mass spectrum at 10 eV indicates that rapid fragmentation of the parent ion occurs at this incident photon energy. Fig. 3(a) gives the initial part the photoion yield curve of the $m/z = 75$ ion, from which we determine the ionization energy of glycine-h_5 to be IE = 9.02 ± 0.02 eV. The corresponding value for glycine-d_5 is IE = 9.07 ± 0.03 eV (Fig. 3(b)). The small increase with respect to glycine-h_5 indicates that the zero-point energy of the glycine ion is less than that of the corresponding neutral molecule, i.e. that at least some of the ion ground state vibrational frequencies are diminished with respect to the neutral ground state values. The ion counts in the ion yield curves for glycine-h_5 under 10 eV photon impact are about seven times weaker than for the corresponding curves for glycine-d_5 under 20 eV photon excitation. In the glycine-d_5 case the S/N is good enough to reveal, in the parent ion curve (Fig. 3(b)), the existence of inflections at energies corresponding to the first seven successive vertical ionization energies IE_v of glycine up to about 16 eV. The 10 successive IE_v values, measured by photoelectron spectroscopy (PES) [21], and the nature of the corresponding molecular orbital of the photoejected electron, when known, are: $IE_v(1) = 10.0$ eV (n_N); $IE_v(2) = 11.1$ eV (n_O); $IE_v(3) = 12.2$ eV (π_{OO}); $IE_v(4) = 13.6$ eV (π_{CH_2}); $IE_v(5) = 14.4$ eV; $IE_v(6) = 15.0$ eV; $IE_v(7) = 15.6$ eV; $IE_v(8) = 16.6$ eV; $IE_v(9) = 16.9$ eV; $IE_v(10) = 17.6$ eV. We note also an inflection in the parent ion curve in the 12.7 eV region, which has no corresponding PES feature (although there is a sharp PES band at 12.7 eV, observed by both Cannington and Ham [21] and by Debies and Rabalais [22] and assigned by the latter authors, without discussion, to a HCl impurity). Another inflection in the PIMS curve occurs at 20.3 eV, which may be associated with ionization of a carbon 2s electron since C 2s bands are observed in this region by HeII PES [21].

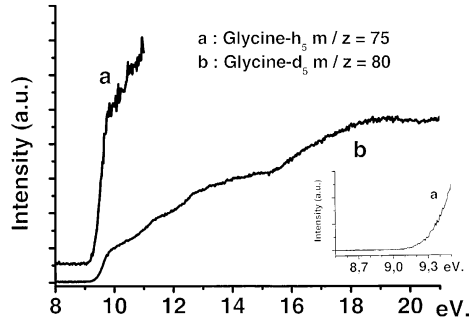

Fig. 3. Photoion yield curves: (a) glycine-h_5, $m/z = 75$ (LiF filter used); (b) glycine-d_5, $m/z = 80$.

Similar inflections were observed in the yield curves of the principal ion fragment in both glycine-h_5 ($m/z = 30$, $NH_2CH_2^+$) and glycine-d_5 ($m/z = 34$, $ND_2CD_2^+$), as discussed later.

There are at least eight possible conformers of glycine, due to internal rotation about the carbon–nitrogen, carbon–carbon and the carbon–oxygen single bond, three of which are stable in the gas phase [23–25]. These three conformers are distinguished by different intramolecular hydrogen-bonding situations arising from the

internal rotations. Previous studies [23–25] indicate that at the temperature of our experiment most of the gas phase glycine molecules will be in one conformer structure, in which a bifurcated interaction links the amino hydrogens to the carbonyl oxygen, and which will be the dominant structure at interstellar temperatures.

Calculations made on the structures and energies of neutral glycine and its radical cation [26] confirm our suggestion that the zero-point energy is smaller in the ion than in the neutral glycine-h_5. In the most stable ion of formula $NH_2CH_2COOH^+$, both the positive charge and the unpaired spin density are localized to the NH_2 group and there is a strong hydrogen bonding interaction between one atom of the NH_2 group and the carboxyl O atom. However, the ion whose formula is $NH_2CHC(OH)_2^+$, in which there are two hydroxy groups, is calculated to be a far more stable isomer. Such carbon-centered radicals, which have both π donor (NH_2) and π acceptor ($C(OH)_2^+$) substituents, have been shown to be more stable than with either substituent alone [27], the extra stabilization giving rise to the so-called "captodative effect" [28]. The formation of the $NH_2CHC(OH)_2^+$ ion by ionization of the neutral NH_2CH_2COOH would require structural reorganisation, including hydrogen migration. The energy barrier for this process is calculated to be of the order of 1.8 eV [29]. If indeed this isomeric ion was formed, fragmentation of its central carbon–carbon bond would lead to fragment ions of $m/z = 29$ and 46 for glycine-h_5 and $m/z = 32$ and 48 for glycine-d_5. The mass spectral results (Table 1) show that formation of the $NH_2CHC(OH)_2^+$ ion is not a significant process. The calculated ionization energy for glycine [$NH_2CH_2COOH \rightarrow NH_2CH_2COOH^+$] is variously reported to be 9.26 eV [26], 9.0 eV, 9.1 eV [30] and 8.8 eV [29], which are all in reasonable agreement with our experimental value 9.02 eV, and which confirms that the ionization process is indeed $NH_2CH_2COOH \rightarrow NH_2CH_2COOH^+$.

Our IE values are the first measured for glycine by direct photoionization techniques. We can compare them with those obtained by electron impact mass spectrometry. Svec and Junk determined a value $IE = 9.25 \pm 0.1$ eV by the vanishing current observation technique [31], while Zaretskii et al. [32] reported a value of 9.21 ± 0.05 eV, from a semi-logarithmic plot of the ionization curve. Our photon impact value is ≈200 meV smaller than the electron impact values, the difference being probably due to better instrumental detection efficiency in our case. The ionization energies values obtained by photoelectron spectroscopy are 10 eV for vertical ionization [21,22]. An adiabatic value of 8.8 eV, given by Debies and Rabalais [22], has a probable error of several tenths of an eV, as judged from the glycine He I PES reported in their Fig. 1. A PES value of 9.00 ± 0.05 eV, measured by Vilesov, is reported by Zaretskii et al. [32], but the reference given in that paper to Vilesov's study does not contain these measurements.

The first ionization energy in glycine is associated with the pyramidal nitrogen atom lone pair orbital, as it is in the related molecule methylamine NH_2CH_3. The ionization energy of the latter is 8.97 ± 0.02 eV [20], which is only slightly less than the value for glycine, indicating that the carboxyl group has relatively little effect on the energy of the nitrogen lone pair orbital, in contrast to inferences that have been drawn from the photoelectron spectra [21,22] and from calculations [26].

3.1.2. The fragment ion $NH_2CH_2^+$: $m/z = 30$

The most intense peak in the glycine-h_5 10 eV photon impact mass spectrum is $m/z = 30$, as is also the case in the 70 eV electron impact spectrum. The possible ion fragment assignments of $m/z = 30$ peaks are $NH_2CH_2^+$, CH_3NH^+ and H_2CO^+. In the mass spectrum of glycine-d_5, measured at a photon energy of 20 eV, the most intense peak is at $m/z = 34$. Correspondingly, the most intense peak in the electron impact mass spectrum of glycine-d_3 is $m/z = 32$ [11]. From these isotopologue results we conclude that the $m/z = 30$ peak in glycine-h_5 is due to the aminomethyl radical ion, $NH_2CH_2^+$, which can be formed by simple bond rupture from $NH_2CH_2COOH^+$, with loss of the COOH group and, furthermore, that there is no prior scrambling of hydrogen atoms, at least involving the hydrogen atom attached to the carbonyl group. Formation of the isomer CH_3NH^+ is less likely since this species is 88 kJ/mol less stable thermodynamically [20] and its formation would require considerable rearrangement either of the parent ion or of the $NH_2CH_2^+$ fragment. The third possible assignment, to H_2CO^+, is excluded since the corresponding ion in glycine-d_5, D_2CO^+, should give rise to a strong peak at $m/z = 32$, whereas this mass peak is weak in the in glycine-d_5 spectrum (Table 1).

Fig. 4 shows the glycine-h_5: $m/z = 30$ ion yield curve (a) and that of the corresponding glycine-d_5 fragment ion $m/z = 34$ (b), both observed using a LiF filter. From semi-log plots of the yield curves we determined the appearance energy of the $m/z = 30$ ion in glycine-h_5 as

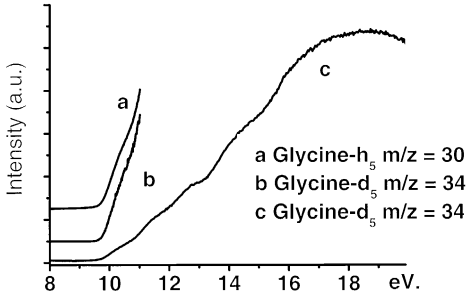

Fig. 4. Photoion yield curves: (a) glycine-h_5, $m/z = 30$ (LiF filter used); (b) glycine-d_5, $m/z = 34$ (LiF filter used); (c) glycine-d_5, $m/z = 34$.

$AE = 9.38 \pm 0.05$ eV and that of the $m/z = 34$ ion in glycine-d_5 as $AE = 9.50 \pm 0.05$ eV, the sign of the difference being the same as that of the ionization energy difference between the parent ion isotopologues.

Loss of the HOCO radical is calculated to be the lowest energy ion fragmentation process [29]. Using the thermochemical data on the heats of formation of glycine, the HOCO radical and the $NH_2CH_2^+$ ion [33], we calculate the expected appearance energy of the ion to be 9.78 eV, which is about 400 meV above our observed value. This difference may be due in part to internal thermal energy in the glycine molecule (estimated as ≈150 meV at 150 °C) but it also points to possible overestimation of the heat of formation of the $NH_2CH_2^+$ ion, determined previously by appearance energy measurements [33], and or of the glycine molecule, and/or underestimation in the heat of formation of the HOCO radical [34]. Indeed, using the earlier value of Ruscic et al. [35] $\Delta H_f(HOCO) = -223$ kJ/mol, the calculated thermochemical appearance energy of the $NH_2CH_2^+$ ion becomes 9.46 eV, in excellent agreement with our observed appearance energy. We note, however, that the combined uncertainties in the values of these various heats of formation are probably of the order of 0.25 eV, so that the agreement between experimental and thermochemical appearance values is in any case reasonable. The reported AE values for the $m/z = 30$ ion in electron impact studies, 10.23 ± 0.09 eV [31] and 10.27 ± 0.05 eV [32], are somewhat higher than our photon impact values, as was found for the parent ion. We remark that the ionization energy of neutral NH_2CH_2 has been determined as IE = 6.29 eV [20]. This low ionization energy is consistent with the relative intensities of the $NH_2CH_2^+$ and $HOCO^+$ ions (Table 1) since HOCO has a much higher ionization energy, as discussed below in Section 3.1.4.

As mentioned previously, the $m/z = 30$ ion yield curve in glycine-h_5 and that of the corresponding fragment ion $m/z = 34$ ion in glycine-d_5 (Fig. 4(c)) exhibit inflections at energies corresponding to the ionization energies of glycine, just as was found for the parent ion curve. This indicates that at the opening up of each new state population there is a modification in the energy deposition distribution in the ion states of the target species, reflected in similar fashion in the principal fragmentation process since the parent ion is relatively unstable.

3.1.3. The fragment ion $HCNH^+$: $m/z = 28$

The second most intense peak in the glycine-h_5 mass spectrum is at $m/z = 28$. This can be assigned to $HCNH^+$ with the aid of the glycine-d_5 mass spectrum, where there is a peak of similar relative intensity at $m/z = 30$, corresponding to $DCND^+$. There are three possible isomers having $m/z = 28$ in the hydrogen case: $HCNH^+$, H_2CN^+ and CNH_2^+. Our choice of $HCNH^+$ is based on calculations of their lowest energy stable forms [36,37] which indicate that H_2CN^+ and CNH_2^+ are respectively 502 and 230 kJ/mol less stable than $HCNH^+$. The onset for formation of $HCNH^+$ ($DCND^+$) is difficult to determine since the $m/z = 28$ (h_5) and $m/z = 30$ (d_5) ion yield curves rise slowly from about 7 eV, becoming more pronounced in the neighbourhood of 9–9.2 eV for both isotopologues (Fig. 5), quite close to the parent IE, but lower than the 9.35 (9.48) eV onset for the $NH_2CH_2^+$ ($ND_2CD_2^+$) ions so that the latter, if produced by the reaction $NH_2CH_2COOH^+ \rightarrow NH_2CH_2^+ + COOH$, cannot be its progenitor in the threshold region. A second, more intense, onset of the $m/z = 28$ (h_5) and $m/z = 30$ (d_5) ion yield curves is observed at 13.0 ± 0.1 (13.1 ± 0.1) eV (Fig. 5). We remark that the $m/z = 28$ ion onsets cannot be due to a carbon monoxide impurity, (which can be formed by thermolysis of glycine), since the ionization energy of CO is 14.014 eV [20], which is almost 5 eV above the first onset of the $m/z = 28$ ion and close to 1 eV above the second onset.

Loss of COOH and H_2 by the glycine ion would lead to a calculated thermochemical appearance energy, $AE(HCNH^+) = 11.88$ eV, which is well above the AE at low energy observed for glycine-h_5 and glycine-d_5 but a little below the 13 eV second observed onset. The low observed first onset may indicate an overestimation of the heat of formation of $HCNH^+$ or that some unusual fragmentation process e.g. $NH_2CH_2COOH^+$ dissociation to $HCNH^+ + HC(OH)_2$ or, more probably, the ion pair formation process $NH_2CH_2COOH \rightarrow HCNH^+ + HC(OH)_2^-$, has occurred. The relevant energetics are unknown. The possibility that the low energy portion of the $m/z = 28$ (h_5) and 30 (d_5) curves are due to second order radiation effects was also considered but was rejected since the $m/z = 30$ (d_5) yield measured with a LiF filter gave a curve which could be followed down to about 7.0 eV, thus supporting the suggestion of an ion pair formation process.

We also considered whether the observation of more than one onset for this fragment ion could be due to formation of one or other of the other two isomers that have been discussed for a $m/z = 28$ species [38]. Ener-

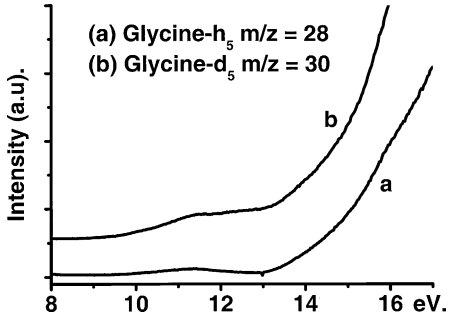

Fig. 5. Photoion yield curves: (a) glycine-h_5, $m/z = 28$; (b) glycine-d_5, $m/z = 30$.

getically, CNH_2^+ would be possible but not H_2CN^+ [36,37,39]. Alternatively, since this second onset is at about 3.6 eV above the onset of for $NH_2CH_2^+$ formation, it could correspond to the formation of $HCNH^+$ by elimination of H_2 from the primarily formed $NH_2CH_2^+$ fragment. However, this would involve first of all isomerisation of $NH_2CH_2^+$ to the transient species CH_3NH^+, which is calculated to be 383 kJ/mol less stable [36]. The potential energy barrier between $NH_2CH_2^+$ and CH_3NH^+ is calculated to be 416 kJ/mol (=4.31 eV). Since we observe the formation of $HCNH^+$ at energies less than the AE = 9.50 eV for $NH_2CH_2^+$, the formation of $HCNH^+$ by loss of H_2 from $NH_2CH_2^+$ is not the $HCNH^+$ formation pathway, at least in the low energy region, as stated above, whereas at the second onset, the intermediate isomerisation process would correspond to a potential energy barrier of the order of 380 kJ/mol, which is only 10% less than that calculated by Øiestad and Uggerud [40]. We remark that their dynamics calculations indicate that the passage over the CH_3NH^+ potential energy region is so fast that there is no time for interchange of the hydrogen atoms, so that the whole dissociation process becomes equivalent to a specific 1,2 H_2 elimination despite the isomerization of $NH_2CH_2^+$ to CH_3NH^+. That hydrogen interchange can occur at some stage in the route to formation of $HCNH^+$ is suggested by the observation in the glycine-d_3 mass spectrum [11] of ion peaks (% relative intensities in brackets) at $m/z = 28$ (9), 29 (21) and 30 (13), which could correspond respectively to $HCNH^+$, $HCND^+$ and $DCND^+$.

The above considerations lead us to consider another possible process that could account for the low energy onset. This involves an initial ion pair dissociation process which can be formed by simple bond rupture from $NH_2CH_2COOH \rightarrow NH_2CH_2^+ + COOH^-$ followed by the dissociation $NH_2CH_2^+ \rightarrow HCNH^+ + H_2$. The long weak tails below 9.5 eV in the $m/z = 30$ (h_5) and $m/z = 34$ (d_5) ion yield curves are consistent with this possibility, since the electron affinity of HOCO is EA = 3.17 ± 0.13 eV [20].

Still another possible pathway for formation of $HCNH^+$ involves the prior formation of metastable NH_2CH^+ ($m/z = 29$), which can dissociate to $HCNH^+ + H$, as shown by Burgers et al. [38], in agreement with the calculations of Uggerud and Schwarz [36], and not to $CNH_2^+ + H$ as proposed earlier [41]. A peak at $m/z = 29$ is observed in the 70 eV electron impact mass spectrum (Table 1) but not in our 10 eV photon impact spectrum. A corresponding peak for ND_2CD^+ was observed at $m/z = 32$ with 20 eV photon impact (Table 1).

We remark that $HCNH^+$ is observed in several galactic sources in the ISM, in particular in the massive star-forming molecular cloud Sgr B2 [42], in which glycine has also recently been detected [5], and that it is also a major ion in the ionosphere of Titan [43]. Electron capture by this ion is thought to be an important reaction forming HCN (+H) and HNC (+H) in dark molecular clouds [39,42], these two molecules being considered to be important in the synthesis of several organic molecules in the ISM. Our observations show that $HCNH^+$ is an important product of the dissociative ionization of glycine. Its initial appearance energy is below 9 eV, so that it could be formed by dissociative ionization of glycine in HI regions where the upper energy limit is 13.6 eV. Thus further radioastronomical searches for glycine should explore regions close to where $HCNH^+$ is observed but where it is reasonably shielded from strong VUV radiation and where it is unlikely that $HCNH^+$ is formed by other means.

3.1.4. The fragment ion $HOCO^+$: $m/z = 45$

A fragment ion is present at $m/z = 45$ in the electron impact mass spectrum of glycine-h_5. There is a corresponding peak at $m/z = 46$ in the 20 eV photoionization mass spectrum of glycine-d_5 (Table 1) and in the electron impact mass spectrum of glycine-d_3 [11]. In the assignment of $m/z = 45$ there is a choice between the hydroxyoxomethylium ion $HOCO^+$ (which in this paper will often be written as $COOH^+$) and the formyloxylium ion $HCOO^+$. The ionization energy of HOCO is $\leqslant 8.195 \pm 0.022$ eV and probably as low as 8.06 ± 0.03 eV [34]. The $HCOO^+$ ion is less stable than the $HOCO^+$ ion by about 1.2 eV [35] and its formation from glycine would require structural rearrangements, not evidenced by the glycine-d_3 mass spectrum, whereas $HOCO^+$ can result from a simple carbon–carbon bond rupture. We therefore assign the $m/z = 45$ peak to $HOCO^+$. The calculated thermochemical value of its appearance energy is 11.8 eV. The relative weakness of the $HOCO^+$ ($DOCO^+$) ion current made it difficult to determine an accurate appearance energy for this fragment ion.

We note that the $HOCO^+$ ion has been observed in the ISM, in the Galactic center region, with a high concentration over several arcmin in Sgr B2 [44]. It has also been observed towards the Sgr A molecular cloud complex [45]. $HOCO^+$ is usually considered to be the protonated form of CO_2 and to be a tracer for CO_2. However, our observations show that it could also be an indicator of the presence of glycine since it can be formed by simple carbon–carbon bond rupture of the glycine cation. Indeed, the $HOCO^+$ ion was observed in interstellar regions where millimeter-wave emission of glycine was recently detected [5].

3.1.5. Other fragment ions of glycine-h_5

3.1.5.1. m/z = 44. This ion is assigned as CO_2^+ and not CH_3CHO^+ or c-$C_2H_4O^+$. The CO_2^+ ion has a calculated thermochemical appearance energy of 13.5 eV if it were a primary fragment formed by the reaction

$NH_2CH_2COOH^+ \rightarrow NH_2CH_3 + CO_2^+$. However, it is largely an impurity in the 20 eV photon impact mass spectrum as evidenced by our observation of a sharp rise of the glycine-d_5 $m/z = 44$ ion yield curve at 13.77 eV and features characteristic of CO_2^+ [46] in the 14.9 and 16.4 eV regions of this curve.

3.1.5.2. m/z = 31. This ion is due in part to $NH_2{}^{13}CH_2^+$ and, in part, to $NH_2CH_3^+$. The shape of the broad weak peak in the $m/z = 36$ region of the glycine-d_5 mass spectrum indicates that it has as components both $m/z = 35$ and $m/z = 36$, which correspond respectively to $ND_2{}^{13}CD_2^+$ and $ND_2CD_3^+$. Further confirmation of these assignments is given by the glycine-d_3 mass spectrum [11] which contains weak peaks at $m/z = 33$ and 34, respectively.

3.1.5.3. m/z = 29. This ion is NH_2CH^+ rather than HCO^+. The mass spectrum of glycine-d_5 supports this assignment from its $m/z = 32$ peak. The glycine-d_3 mass spectrum has its most intense peak at $m/z = 32$, due to $ND_2CH_2^+$, so that this spectrum cannot be used to further confirm the $m/z = 29$ assignment to NH_2CH^+ in glycine-h_5.

3.1.5.4. m/z = 27. $m/z = 27$, which is observed with 70 eV electron excitation of glycine-h_5, is possibly HCN^+ but the corresponding DCN^+ ion is not observed at $m/z = 28$ in the 20 eV photon energy impact mass spectrum of glycine-d_5. The calculated thermochemical appearance energy of HCN^+ has a value of 14.57 eV, which is a minimum value but well below 20 eV, so that, if formed, DCN^+ should have been observed in the glycine-d_5 spectrum. The glycine-d_3 mass spectrum in this m/z region is not useful for verifying a HCN^+ assignment. A more probable assignment of $m/z = 27$ is $C_2H_3^+$, which could be formed from the parent ion by loss of both O_2 and NH_2. The $C_2D_3^+$ signal would be masked in glycine-d_5 by the strong $DCND^+$ peak at the same $m/z = 30$ value.

3.1.5.5. m/z = 18. $m/z = 18$ is assigned to the ammonium ion NH_4^+. If this peak were due to H_2O^+ one would expect a change of slope at 12.6 eV in the ion yield curve, which was not observed. Furthermore, the absence of the OH^+ peak at $m/z = 17$ in the 20 eV photon impact mass spectra of glycine-d_5 shows that there is very little H_2O impurity in the latter spectrum. It is unlikely, in glycine-d_5, that the weak peaks at $m/z = 18$ and 20 (Table 1) are due to D_2O impurity; they are more probably due to ND_2^+ and ND_3^+. The $ND_2^+ + CD_2COOD$ product channel is calculated to lie about 15.8 eV [29] and thus well below the 20 eV photon excitation of glycine-d_5. However, the $ND_2 + CD_2COOD^+$ channel is calculated to lie lower still, at about 12.25 eV [29]. Since the CD_2COOD^+ ion ($m/z = 62$) was not observed in the glycine-d_5 mass spectrum (Fig. 2), nor is the CH_2COOH^+ ion ($m/z = 59$) observed in electron impact mass spectra of glycine-h_5, it is more likely that ND_2^+ (and ND_3^+) result from dissociation of ND_4^+.

The spectrum of glycine-d_5 (Table 1, Fig. 2) and the 70 eV electron impact mass spectrum of glycine-d_3 [11] are consistent with the NH_4^+ assignment proposed above. The $m/z = 18$ peak in glycine-h_5 is shifted to $m/z = 22$ in glycine-d_5, while in glycine-d_3, it is shifted to $m/z = 20$ [11]. The inference from the glycine-d_3 spectrum is that in glycine-h_5 the NH_4^+ ion contains the two amino hydrogens and two hydrogens originally attached to the carbon skeleton. The appearance energy of the ND_4^+ ion in glycine-d_5 is at 13.4 ± 0.1 eV. It is of interest that the NH_4^+ ion is observed in the mass spectra of many amino acids [11], amines, and other nitrogenous compounds [47].

Finally, we remark that the peak at $m/z = 33$ in the 20 eV photon impact mass spectrum of glycine-d_5, which has a quite important relative intensity, is probably due to an isotopic impurity. A possible assignment is to the ND_2CHD^+ or $NHDCD_2^+$ fragment resulting from a glycine-hd_4 impurity in the Sigma-Aldrich sample, which had a stated deuterium purity of 97%. The observation of a significant peak at $m/z = 33$ in the glycine-d_3 mass spectrum [11] is consistent with the our isotopic impurity interpretation in the glycine-d_5 case.

3.2. α-Alanine $NH_2CH_3CHCOOH$ (elemental composition: $C_3H_7NO_2$)

The amino acid α-alanine $NH_2CH_3CHCOOH$ can exist in at least 13 different conformer structures in the gas phase [48]. The replacement by a CH_3 group of one of the hydrogen atoms in the CH_2 group of glycine (Fig. 1) gives rise to α-alanine conformers which, with respect to glycine, are little different in geometry or in preference as to the most stable conformers. One conformer, in which the nitrogen atom of the amino group is in the *syn* position to the carbonyl oxygen, dominates in the gas phase [48–50]. In our experiments we used enantiomeric mixtures of the D- and L-forms of the chiral molecule α-alanine.

Table 2 lists the m/z values and the relative peak intensities of the mass spectrum of α-alanine (Fig. 2) obtained at a photon energy of 20 eV. The peaks are the same as those observed with 70 eV electron impact [11] and their relative intensities are generally very similar.

3.2.1. The parent ion $NH_2CH_3CHCOOH^+$: m/z = 89

The ionization energy of α-alanine was measured from the $m/z = 89$ ion yield curve (Fig. 6). The semi-log plot gave an onset value $IE = 8.75 \pm 0.05$ eV. This IE value, measured for the first time by photon impact mass spectrometry, is a little lower than He I PES values reported by Klasinc [51], $IE(ad) = 8.88$ eV for the adia-

Table 2
α-Alanine: $NH_2CH_3CHCOOH$

m/z	Electron impact 70 eV [11] relative intensity	Photon impact 20 eV relative intensity	Photon impact AE/eV	Ion assignments
89	0.2	2	8.75 ± 0.05	$NH_2CH_3CHCOOH^+$
74	2	1	9.3 ± 0.2	$NH_2CHCOOH^+$
55	1	1		See text
45	7	5		$HOCO^+$
44	100	100	9.05 ± 0.10	$NH_2CH_3CH^+$
43	4	4		$NH_2CH_2CH^+$
42	12	12		$NH_2CH_2C^+$
30	1	4		$NH_2CH_2^+$
29	4	6		NH_2CH^+
28	20	41	12.35[a]	$HCNH^+$
27	6	10	11.5 ± 0.2	$C_2H_3^+$
18	24	85	12.0[a]	NH_4^+
				H_2O^+[a]
15	6	4		CH_3^+

Mass spectra and appearance energies. Ion assignments of m/z peaks.
[a] See text.

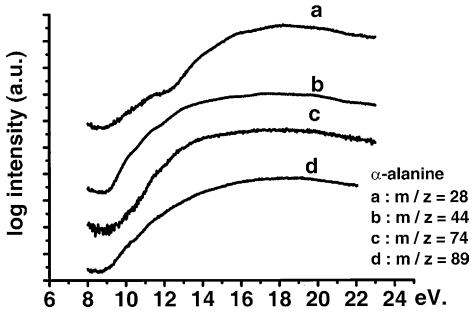

Fig. 6. Semi-log plots of photoion yield curves of α-alanine: (a) $m/z = 28$; (b) $m/z = 44$; (c) $m/z = 74$; (d) $m/z = 89$.

batic IE (9.77 eV for the vertical IE), and by Debies and Rabalais [22], IE(ad) = 8.8 eV, (IE(vert.) = 9.8 eV), while Cannington and Ham [21] give IE(vert.) = 9.85 eV. No electron impact measurements of the IE have been reported for α-alanine.

The lowest appearance energy of fragment ions is for the $m/z = 44$ $NH_2CH_3CH^+$ ion at 9.05 ± 0.10 eV (Fig. 6; Table 2), i.e. of the order of 0.3 eV above the parent ion appearance energy. The weakness of the parent ion peak at 20 eV photon excitation, and its even weaker relative intensity in the 70 eV electron impact mass spectrum [11], indicate that the rate of dissociation of the parent amino acid cation, which begins when its internal energy is of the order of 0.3 eV (or less), is strongly internal energy dependent.

3.2.2. Fragment ions of α-alanine

The principal fragment peaks in both the photon impact and electron impact spectra are $m/z = 44$, 18, 28 and 42, in decreasing order of intensity. The appearance energies of many of the observed peaks were measured and their values are also given in Table 2.

Assignment of the fragment ions in the α-alanine mass spectra listed in Table 2 was assisted by the 70 eV electron impact mass spectra of the isotopologue α-alanine-d_3 reported by Junk and Svec [11]. In this deuterated species the carboxyl and amino hydrogens in α-alanine have been replaced by deuterium.

3.2.2.1. $m/z = 74$. In the α-alanine mass spectra, the $m/z = 74$ ion corresponds to loss of a CH_3 group to form the $NH_2CHCOOH^+$ fragment ion. This glycyl radical cation is calculated to be a stable structure, whereas its carboxylate cation isomer, $NH_2CH_2COO^+$, is predicted to undergo spontaneous dissociation [52]. The glycyl radical cation is easily formed by electron impact on several different amino acids [53]. In our case this radical cation is not a major product either as a stable or as an unstable entity since the ion fragments $m/z = 57$ (loss of OH), 56 (loss of H_2O) and 46 (loss of CO), which are some of the important products of its collisionally induced dissociation [53,54], are either absent or very weak in the electron and photon impact mass spectra of α-alanine (Table 2).

Confirmation of the assignment of the $m/z = 74$ ion to $NH_2CHCOOH^+$ is provided by the observation of a corresponding peak, of similar relative intensity, at $m/z = 77$ in the α-alanine-d_3 electron impact mass spectrum [11], indicating that both the amino and the carboxyl hydrogens of α-alanine are present in the $NH_2CHCOOH^+$ ion.

The measured appearance energy of the $m/z = 74$ ion in our PIMS study is AE = 9.3 ± 0.2 eV (Fig. 6, Table 2). This leads to a thermochemical determination of the upper limit for the heat of formation of the $NH_2CHCOOH^+$ ion, $\Delta H_f \leqslant 333 \pm 20$ kJ/mol.

Concerning the two reactions (i) $NH_2CH_3CHCOOH^+ \rightarrow NH_2CHCOOH^+ + CH_3$ and (ii) $NH_2CH_3CHCOOH^+ \rightarrow NH_2CHCOOH + CH_3^+$, which both involve simple bond rupture between the carbon of the methyl group and the adjacent carbon atom, and are

competitive, we remark that the relatively low yields of $NH_2CHCOOH^+$ ($m/z = 74$) and of CH_3^+ ($m/z = 15$) indicate that the positive charge on the parent ion is localised preferentially on the nitrogen and adjacent carbon atoms. The corresponding reaction of $NH_2CHCOOH^+$ formation in glycine, by loss of an H atom from the CH_2 group, was not observed in our photon impact study.

3.2.2.2. $m/z = 44$. The principal fragment ion is $m/z = 44$, which corresponds to the $NH_2CH_3CH^+$ ion formed by loss of the COOH radical in a simple bond rupture process: $NH_2CH_3CHCOOH^+ \rightarrow NH_2CH_3CH^+ + HOCO$. Its appearance energy, 9.05 ± 0.10 eV (Fig. 6, Table 2), is very close to the thermochemical value 9.12 eV which we calculated from heat of formation data [33]. The relative intensities of the $m/z = 44$ and $m/z = 45$ ions indicate that this reaction appears to be favoured over the competitive reaction $NH_2CH_3CHCOOH^+ \rightarrow NH_2CH_3CH + HOCO^+$). As mentioned previously, the HOCO (=COOH) species has an ionization energy of 8.06 eV [34]. The Stevenson–Audier–Harrison (SAH) rule [55–57] implies that for an odd-electron monocation dissociating into two products, one of which is itself an ion, the preferred reaction would be that for which the neutral fragment has the higher ionization energy It is therefore not unexpected, from the SAH rule, that the ionization energy of the NH_2CH_3CH species, 6.1 eV [20], is considerably lower than that of HOCO.

We note that in the electron impact mass spectrum of α-alanine-d_3 [11], the principal ion peak is at $m/z = 46$. We assign it as mainly due to the $ND_2CH_3CH^+$ ion and, judging from the corresponding α-alanine mass spectrum peak intensities, in small part to the $DOCO^+$ ion. The high intensity of the $m/z = 46$ peak in the α-alanine-d_3 mass spectrum confirms the assignment of the $m/z = 44$ peak in the α-alanine-h_7 mass spectrum as being due to the $NH_2CH_3CH^+$ ion. The mass spectra of the two isotopologues also indicate that the carboxyl hydrogen does not migrate before carbon–carbon rupture takes place to form the fragment ion.

3.2.2.3. $m/z = 42, 43, 45$. The most probable assignment of the $m/z = 42$ ion is to the $NH_2CH_2{=}C^{\cdot+}$ radical ion. This is supported by the observation of a reasonably intense $m/z = 44$ ($ND_2CH_2{=}C^{\cdot+}$) peak in the α-alanine-d_3 electron impact mass spectrum [11]. The fragment ion $m/z = 43$ is assigned to $NH_2CHCH_2^+$ resulting from loss of formic acid HCOOH. This involves hydrogen migration since it cannot be formed by a simple bond rupture process. The calculated thermochemical value of its appearance energy, 8.87 eV, is close to the observed IE of α-alanine. The $m/z = 45$ ion is undoubtedly the $HOCO^+$ species, formed by simple rupture of the central C–C bond.

3.2.2.4. $m/z = 30$. The formation of $NH_2CH_2^+$ ($m/z = 30$) probably involves dissociation of a primary product ion. The latter could be the $m/z = 74$ unstable carboxylate ion $NH_2CH_2COO^+$, which might be formed along with its stable immonium isomer $NH_2CHCOOH^+$. O'Hair et al. [52] predict the dissociation to be $NH_2CH_2COO^+ \rightarrow NH_2CH_2^+ + CO_2$. Because of the high IE of CO_2, 13.77 eV [46], this dissociation pathway is more probable than that leading to the carbon dioxide cation, $NH_2CH_2COO^+ \rightarrow NH_2CH_2 + CO_2^+$.

3.2.2.5. $m/z = 29$. The $m/z = 29$ ion could be either HCO^+ or NH_2CH^+. The α-alanine-d_3 mass spectrum is of little assistance in helping us to choose between these two possible assignments. The formation of these ions requires the breaking of two bonds in α-alanine, the central C–C and the C=O bonds in the case of HCO^+ and the C–C and C–CH_3 bonds in the case of NH_2CH^+. We note that the corresponding latter reaction in glycine, $NH_2CH_2COOH^+ \rightarrow NH_2CH^+ + H + COOH$ was observed in both 20 eV photon impact (deuterated version, Table 1) and in 70 eV electron impact experiments. This encourages us to assign $m/z = 29$ to the NH_2CH^+ ion. Furthermore, a $(P–R–COOH)^+$ ion at $m/z = 29$, in which the parent amino acid species (P) loses the alkyl radical R and the COOH group, is observed in a series of amino acid electron impact mass spectra and was assigned to NH_2CH^+ [11].

3.2.2.6. $m/z = 28$. The $m/z = 28$ ion is an intense fragment ion. It is undoubtedly $HCNH^+$ and its yield curve (Fig. 6) exhibits an initial onset at 9.0 ± 0.1 eV and a sharp rise in signal at 12.35 eV, which we consider as a second onset energy. As in the case of glycine, there appear to be two separate processes forming this ion, the higher energy one prossibly involving loss of H_2 from primarily formed $NH_2CH_2^+$. The α-alanine-d_3 mass spectrum contains a spread of m/z values in the 28–30 range, the most intense being at $m/z = 29$ (relative intensity 17%), which suggests that there is significant hydrogen migration in the processes leading to the formation of $HCNH^+$, similar to the case of its formation in glycine (cf. Section 3.1.3). Several pathways are possible, analogous to those discussed in the case of glycine in Section 3.1.3.

3.2.2.7. $m/z = 27$. The $m/z = 27$ ion can be assigned to the $C_2H_3^+$ ion rather than to HCN^+. This assignment, which corresponds to loss of COOH and NH_3 neutrals, is confirmed by the α-alanine-d_3 electron impact mass spectrum which exhibits a peak of similar intensity at $m/z = 27$ ($C_2H_3^+$). No mass shift is expected for the $C_2H_3^+$ fragment in an α-alanine system in which the carboxyl and amino hydrogens have been replaced by deuterium, since the expected process in α-alanine-d_3 [11] would be $ND_2CHCH_3COOD^+ \rightarrow ND_2CHCH_3^+ +$

COOD, followed by $ND_2CHCH_3^+ \rightarrow C_2H_3^+ + NHD_2$. The measured $AE = 11.5 \pm 0.2$ eV is below the thermochemical estimation 13.2 eV which, however, has been calculated for an unspecified form [20] of $C_2H_3^+$.

3.2.2.8. $m/z = 18$. The $m/z = 18$ ion is assigned as NH_4^+, with HC═CH–COOH as neutral product. The appearance energy in our $m/z = 18$ ion yield curve is in the 12 eV region. In the electron impact mass spectrum of α-alanine-d_3 the strong $m/z = 18$ peak is shifted to $m/z = 20$ [11]. This is consistent with (i) the $m/z = 20$ ion being $ND_2H_2^+$ in this isotopologue, where it is 32% as intense as the principal ion peak ($m/z = 46$) and (ii), the $m/z = 18$ ion in α-alanine as being NH_4^+. It also shows that the NH_4^+ ion contains the two amino hydrogens and two hydrogens originally attached to the carbon skeleton. Formation of the NH_4^+ ion involves rearrangement processes [11] but the hydrogen atom attached to the carboxyl group is not favoured as a participating migrant species since in the α-alanine-d_3 electron impact mass spectrum, the $m/z = 21$ ion, corresponding to an ammonium ion containing all three deuterium atoms, is only 2% as intense as the principal ion peak.

We note that there was no change of slope at 12.6 eV in the $m/z = 18$ photoion yield curve. This, coupled with the extreme weakness of the OH^+ peak at $m/z = 17$ in the 20 eV photon impact mass spectrum of α-alanine, shows that there is very little H_2O impurity. In fact, from the relative intensities of the $m/z = 17$:18 peak heights in the mass spectrum we can determine the maximum contribution of H_2O^+ to the $m/z = 18$ peak, given that, for water at 20 eV photon impact, the ratio of the intensities of the $m/z = 17$ (OH^+) and $m/z = 18$ (H_2O^+) peaks is 0.33 [46]. In the case of α-alanine, the maximum contribution of H_2O^+ to the $m/z = 18$ peak is 5%. This is a maximum value since we have neglected any possible contribution of the NH_3^+ ion to the $m/z = 17$ ion peak.

3.2.2.9. $m/z = 55$. We have not been able to make an assignment of the weak ion peak at $m/z = 55$. It could be the propargylamine cation $H_3C–C{\equiv}C–NH_2^+$ but its formation would involve considerable rearrangements of the atoms and this requires further work for confirmation.

3.3. β-Alanine $NH_2(CH_2)_2COOH$ (elemental composition: $C_3H_7NO_2$)

The rotational spectrum of gas phase β-alanine has been assigned to two conformers having *gauche* conformations and which involve the same types of intramolecular interactions that occur in glycine and in α-alanine [58]. The energy difference between these two conformers is not known, so we cannot evaluate the conformer content of our gas phase sample.

Table 3 lists the m/z values and the relative peak intensities of the mass spectrum of β-alanine obtained at a photon energy of 20 eV (Fig. 2), and which are very similar to those observed with 70 eV electron impact [20].

Table 3
β-Alanine: $NH_2(CH_2)_2COOH$

m/z	Electron impact 70 eV [20] relative intensity	Photon impact 20 eV relative intensity	Photon impact AE/eV	Ion assignments
89	5	2	8.8 ± 0.1	$NH_2(CH_2)_2COOH^+$
72	1	1		$NH_2(CH_2)_2CO^+$ or $(CH_2)_2COO^+$
70	4	3		$NH_2CHCHCO^+$
60	1	1		CH_3COOH^+
55	1	1		See text
45	2	5		$HOCO^+$
44	3	4		$NH_2(CH_2)_2^+$
43	6	10	9.5 ± 0.2	$NH_2CHCH_2^+$
42	4	7		$NH_2CH_2{=}C^{\cdot+}$
31	1	1		$NH_2{}^{13}CH_2^+$
30	100	100	9.3 ± 0.1[a]	$NH_2CH_2^+$
29	1	1		NH_2CH^+
28	7	10	14.2 ± 0.1[a]	$HCNH^+$
27	N/A	3		$C_2H_3^+$
18	N/A	17		NH_4^+
				H_2O^+[b]
15	N/A	3		CH_3^+

Mass spectra and appearance energies. Ion assignments of m/z peaks.
[a] This ion yield curve also has a low energy tail, see text.
[b] See text.

3.3.1. The parent ion $NH_2(CH_2)_2COOH^+$: $m/z = 89$

The ionization energy of β-alanine was measured from the $m/z = 89$ ion yield curve. The curve in the threshold region has a sharp onset (Fig. 7) giving IE = 8.8 ± 0.1 eV. No IE values for β-alanine are reported in the NIST collection [20]. The first peak in the He I photoelectron spectrum of β-alanine is at 9.7 eV [21]; we estimate its onset at ≈8.7 eV from the PE spectrum given in Fig. 6(a) of Cannington and Ham [21].

The parent ion yield curve rises rapidly from threshold but changes markedly in slope above 9.5 eV which, as seen below, is only a little above the appearance energy, 9.3 ± 0.1 eV of the principal fragment ion $NH_2CH_2^+$ ($m/z = 30$, Fig. 7). The relative weakness of the β-alanine parent ion peak in both photon and electron impact mass spectra indicates, as for the analogous case of α-alanine, that dissociation of the parent amino acid cation requires only a small amount of internal energy.

3.3.2. Fragment ions of β-alanine

The principal fragment peaks in the β-alanine spectra are $m/z = 30$, 18, 28, 43 and 45, in decreasing order of intensity. We discuss these in turn.

3.3.2.1. $m/z = 30$. The most intense peak, at $m/z = 30$ is assigned to the $NH_2CH_2^+$ ion resulting from loss of the CH_2COOH radical by simple rupture of the carbon–carbon bond joining the two CH_2 groups. Its ^{13}C isotopologue is observed at $m/z = 31$. The appearance energy of the $NH_2CH_2^+$ ion is 9.3 ± 0.1 eV which, from available thermochemical data [33], provides a value $\Delta H_f = -272 \pm 10$ kJ/mol for the heat of formation of the CH_2COOH species. The reported experimental value is −257 ± 13 kJ/mol [59], and a calculated value is of the order of −240 kJ/mol [60]. Based on the experimental value for the heat of formation of the CH_2COOH radical, the appearance energy of $NH_2CH_2^+$ is calculated to be AE = 9.44 ± 0.14 eV, i.e. in good agreement with our experimental AE = 9.3 ± 0.1 eV. We note that if CH_2COOH were the isomer CH_3COO then, using its experimental heat of formation $\Delta H_f(CH_3COO) = -217 \pm 13$ kJ/mol [59], the calculated thermochemical value AE ($NH_2CH_2^+$) is 10.49 ± 0.14 eV, i.e. well above the experimental AE = 9.3 ± 0.1 eV. This shows that the neutral product is CH_2COOH and not CH_3COO.

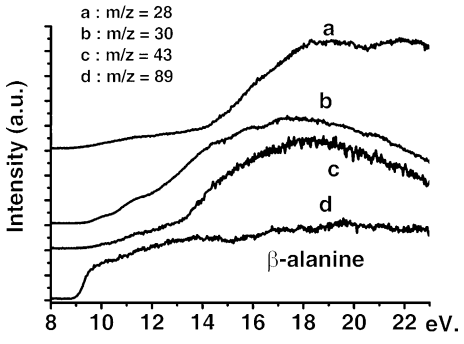

Fig. 7. Photoion yield curves: of β-alanine: (a) $m/z = 28$; (b) $m/z = 30$; (c) $m/z = 43$; (d) $m/z = 89$.

In the $m/z = 30$ ion yield curve there is a weak but long tail down to 7 eV, very clearly observed in measurements made using a LiF filter. This tail could result from the ion pair formation process $NH_2(CH_2)_2COOH \rightarrow NH_2CH_2^+ + CH_2COOH^-$. The electron affinity of CH_2COOH is reported to be EA = 1.87 eV, so that the appearance energy of $NH_2CH_2^+$ formed by the ion pair process can be calculated to be at about 7.4 eV [61], in good agreement with our long tail observation.

We note that in the $m/z = 30$ ion yield curve there are inflections at, or close to, the energies corresponding to the low-energy rise of several peaks in the He I photoelectron spectrum of β-alanine [21], in particular the 9.7 (n_N), 10.75 (n_O), 12.1 (π_{OO}) and 12.7 eV peaks.

3.3.2.2. $m/z = 18$. The $m/z = 18$ peak is assigned to the NH_4^+ ion, requiring hydrogen migration for its formation, as in the case of α-alanine (see above), and the neutral product is suggested here too to be HC═CH–COOH. A change of slope observed at 12.6 eV in the $m/z = 18$ ion yield curve shows that there is indeed some H_2O impurity in this experiment. From the relative strength of the peak at $m/z = 17$ to that of at $m/z = 18$ in the 20 eV photon impact mass spectrum of β-alanine, we estimate the maximum contribution of H_2O^+ to the $m/z = 18$ peak to be 60%.

3.3.2.3. $m/z = 28$. Assignment of the $m/z = 28$ ion peak is to $HCNH^+$. The ion yield curve (Fig. 7) reveals two onset energies, at 9.0 eV and 14.2 ± 0.1 eV, respectively. The calculated thermochemical value of the appearance energy is 11.99 eV for $HCNH^+$. The large increase in intensity of the yield curve at 14.2 eV could be related to dissociation of the $m/z = 30$ ion, i.e. to the process $NH_2CH_2^+ \rightarrow HCNH^+ + H_2$. It is of interest to consider the energy difference ΔE between the second onset of the $m/z = 28$ ion and the AE of the $m/z = 30$ ion in the following series of amino acids: glycine, $\Delta E = 3.62$ eV; α-alanine, $\Delta E \leqslant 3.6$ eV (although the AE for $m/z = 30$ was not measured for α-alanine, it must be greater than or equal to the 8.75 eV ionization energy, so that $\Delta E \leqslant 3.6$ eV); and β-alanine, $\Delta E = 4.9$ eV. The fact that ΔE is more than 1 eV greater in β-alanine than in the other two amino acids could signify that the intermediate species "$NH_2CH_2^+$" has a different structure in α-alanine as compared with β-alanine.

In view of the fact that the ionization energy of carbon monoxide is 14.014 eV [20], another possible interpretation of the second onset is that it is due, at least partially, to a thermally produced CO impurity. How-

ever, the shape of the $m/z = 28$ ion yield curve in the high energy region, which exhibits intensity maxima at ≈19 and ≈21.7 eV, and a minimum at ≈20.6 eV (Fig. 7), differs considerably from the ionization quantum yield (Φ_{ion}) curve of CO, which has a maximum ($\Phi_{ion} \approx 1$) at ≈14.8 eV and a minimum ($\Phi_{ion} \approx 0.5$) at ≈16.3 eV followed by a rise to a plateau ($\Phi_{ion} \approx 1$) at ≈19.1 eV [46], in a spectral region where the photoabsorption cross section varies less than 10% [62]. We therefore consider that the two onset energies for the $m/z = 28$ fragment ion reflect two mechanisms of formation of $HCNH^+$ in β-alanine, as in the cases of glycine and α-alanine discussed previously.

3.3.2.4. $m/z = 42$–45. The $m/z = 42$ ion is possibly the $NH_2CH_2{=}C^{\cdot+}$ radical ion. The $m/z = 43$ peak we consider to correspond to the $NH_2CHCH_2^+$ ion formed by loss of formic acid HCOOH. This involves hydrogen migration since it cannot be formed by a simple bond rupture process. Its onset energy, 9.5 ± 0.2 eV is, indeed, above the calculated thermochemical value, 8.96 eV. The suggested carrier of the $m/z = 44$ ion, $NH_2(CH_2)_2^+$, can be formed by a simple carbon–carbon bond rupture process, leaving HOCO as the neutral fragment, while the $m/z = 45$ ion is undoubtedly $HOCO^+$, formed by simple carbon–carbon bond rupture, in competition with the process forming the $m/z = 44$ ion.

3.3.2.5. Other fragment ions formed by dissociative ionization of β-alanine. There are two possible assignments for the $m/z = 72$ ion, which appears very weakly in both the 20 eV photon impact and the electron impact mass spectra. These are $NH_2(CH_2)_2CO^+$, corresponding to loss of OH, and $(CH_2)_2COO^+$ with loss of NH_3. For $m/z = 70$, the ion is uniquely assigned to $NH_2(CH)_2CO^+$ but here there are two possibilities as to the neutral products $OH + H_2$ or $H_2O + H$. The $m/z = 60$ ion is possibly CH_3COOH^+ (loss of NH_2CH); its isomer, $HCOOCH_3^+$, is much less likely. The $m/z = 29$ ion we assign to NH_2CH^+ rather than to HCO^+, and $m/z = 27$ is assigned to $C_2H_3^+$ rather than to HCN^+. Deuterium isotopologue studies are required to verify or clarify the assignments in all of these cases. Finally, we note that the $m/z = 15$ peak is reasonably assigned to the methyl cation and that, just as in the case of α-alanine, it has not been possible to make a definitive assignment of the weak ion peak at $m/z = 55$.

3.4. Further remarks on the dissociative photoionization of α-alanine and β-alanine

The mass spectra of α-alanine and β-alanine are very different (Fig. 2), the latter being more similar to that of glycine. The $m/z = 30$, $NH_2CH_2^+$ ion, is strongest in β-alanine, as in glycine, whereas $m/z = 44$ $NH_2CH_3CH^+$, the methyl substituted analog of $NH_2CH_2^+$, is strongest in α-alanine. Thus in β-alanine there does not occur rearrangement of $(CH_2)_2$ to the CH_3CH form or, in α-alanine from CH_3CH to $(CH_2)_2$. The $m/z = 29$ ion, NH_2CH^+, is much weaker in β-alanine than in α-alanine because in the latter its formation requires loss of CH_3 and of COOH. If this could occur in β-alanine it would require isomerisation to α-alanine before dissociation. The general difference between the mass spectra of α-alanine and β-alanine shows that this isomerisation does not occur to any noticeable extent.

In β-alanine the major ion $m/z = 30$, $NH_2CH_2^+$, is formed by simple rupture of a carbon–carbon bond, with consequent loss of CH_2COOH, whereas in α-alanine the $m/z = 30$ ion $NH_2CH_2^+$ is a minor product ion, formed by dissociation of a primary fragment ion. The major ion $NH_2CH_3CH^+$ in α-alanine corresponds to P–COOH at $m/z = 44$.

The ion yield curves for the $HCNH^+$ ion at $m/z = 28$ in both α-alanine and β-alanine exhibit characteristics that suggest the possibility of two different mechanisms of formation of this astrophysically important fragment ion in each of the two isomers. The ammonium ion is also of astrophysical importance. From our ion yield results, we determine minimum branching ratios for formation of NH_4^+ at 20 eV photon impact, whose values, 30% for α-alanine and 4.5% for β-alanine, are very different for the two alanines. This indicates that there is greater ease of hydrogen atom migration to the amino group in the case of α-alanine.

We note that both α-alanine and β-alanine ions would be easily photodissociated in HI regions of the interstellar medium since the ion dissociation limits are well below the 13.6 eV HI photon energy limit. Key fragment ions as markers for radioastronomical search for the alanines in space are $NH_2CH_3CH^+$, $HCNH^+$ and NH_4^+ for α-alanine and $NH_2CH_2^+$ for β-alanine. To the best of our knowledge, the $NH_2CH_3CH^+$ and $NH_2CH_2^+$ ions have not been studied in the microwave region. The NH_4^+ ion has been studied in the infrared region, and possibly observed in interstellar ices [63], while the $HCNH^+$ ion has been observed in the laboratory and in the interstellar medium by radiofrequency spectroscopy. Key neutral fragments for radioastronomical search for the alanines are HOCO ($HOCO^+$ is observed in the interstellar medium) for α-alanine, and CH_2COOH for β-alanine [17].

3.5. α-Aminoisobutyric acid $NH_2C(CH_3)_2COOH$ (elemental composition: $C_4H_9NO_2$)

This non-chiral α-amino acid is related to chiral α-alanine via methyl group replacement of the hydrogen atom attached to the α-carbon of the latter (Fig. 1). It is therefore also capable of existing in many conformeric forms but this has been relatively little explored. We note that α-aminoisobutyric acid is not a constituent of

proteins. However, it is one of the most abundant amino acids found in the Murchison meteorite [2] where, by isotopic ratio analysis, it has been shown to be of extraterrestrial origin [64]. It has also been observed in micrometeorites recovered from the Antarctic, in concentrations well above those expected from possible terrestrial contamination [3].

Comparison between our 20 eV photon impact mass spectrum (Fig. 2, Table 4) and the 70 eV electron impact spectrum of Junk and Svec [11] shows that the two most intense ions are the same in each spectrum, i.e. $m/z = 58$ and 42 but that the parent ion at $m/z = 103$ is relatively much weaker in the electron impact mass spectrum. This probably reflects a smaller ion source residence time of the metastable parent ion in our case.

3.5.1. The parent ion α-aminoisobutyric acid $NH_2C(CH_3)_2COOH^+$: $m/z = 103$

From the $m/z = 103$ parent ion yield curve (Fig. 8) we determine the ionization energy of α-aminoisobutyric acid to be 9.6 ± 0.2 eV, which is apparently the first measurement of this entity since there are no reported values in the literature. The heat of formation of α-aminoisobutyric acid has recently been reported as being -459 ± 5 kJ/mol [65]. By combining this value with our observed ionization energy, the heat of formation of the α-aminoisobutyric acid cation has an upper limit of 467 ± 24 kJ/mol.

3.5.2. Fragment ions of α-aminoisobutyric acid

Assignments of fragment ions resulting from dissociative ionization of α-aminoisobutyric acid are given in Table 4, along with the appearance energy values for the principal ions produced by photon impact.

3.5.2.1. $m/z = 88$. The $m/z = 88$ peak is assigned to the $NH_2CCH_3COOH^+$ ion, formed by CH_3 loss. The charge switched reaction $NH_2C(CH_3)_2COOH^+ \rightarrow NH_2CCH_3COOH + CH_3^+$ ($m/z = 15$) is also observed with apparent equal probability.

3.5.2.2. $m/z = 45$ and 58. The principal fragment ion, $m/z = 58$, is assigned to $NH_2C(CH_3)_2^+$, formed by loss of COOH by simple rupture of the C–C bond linking it to the α-carbon. The ion at $m/z = 45$, assigned to $HOCO^+$, is formed by the corresponding charge switch reaction $NH_2C(CH_3)_2COOH^+ \rightarrow NH_2C(CH_3)_2 + HOCO^+$. The relative intensities of the $m/z = 58$ and 45 ions reflect the greater ease of formation of the $NH_2C(CH_3)_2^+$ ion and confirms the SAH rule [55–57], since the ionization energies of $NH_2C(CH_3)_2$ and HOCO are 5.4 eV [20] and 8.06 eV [34], respectively. Our observed appearance energy of the $NH_2C(CH_3)_2^+$ ion, 9.1 ± 0.1 eV (Fig. 8, Table 4), is 0.5 eV below the parent ionization energy, which suggests that in the threshold energy region it is formed by an ion pair dissociation process, $NH_2C(CH_3)_2COOH \rightarrow NH_2C(CH_3)_2^+ + HOCO^-$. The calculated thermochemical appearance energy for this process is less than 6 eV, while that for the dissociative ionization process leading to neutral HOCO is 8.9 ± 0.1 eV, close to the actual appearance energy of the $NH_2C(CH_3)_2^+$ ion.

3.5.2.3. $m/z = 42$. The second most intense fragment ion, at $m/z = 42$, also observed in electron impact mass spectra [11], was assigned in the latter by Junk and Svec to $C_3H_6^+$, of suggested structure $CH_3–C^+–CH_3$ formed by successive loss of COOH and NH_2. The experimental heat of formation of this ion has an upper limit of 1062 kJ/mol and a calculated value of 1053 kJ/mol [66]. Using this latter value in the process $NH_2C(CH_3)_2COOH^+ \rightarrow C_3H_6^+ + COOH$ and NH_2, the calculated thermochemical appearance energy of the $CH_3–C^+–CH_3$ ion is 15.31 and 14.34 eV if the $C_3H_6^+$ ion has the

Table 4
α-Aminoisobutyric acid: $NH_2C(CH_3)_2COOH$

m/z	Electron impact 70 eV [11] relative intensity	Photon impact 20 eV relative intensity	Photon impact AE/eV	Ion
103	0.1	7	9.6 ± 0.2	$NH_2C(CH_3)_2COOH^+$
88	5	2		$NH_2CCH_3COOH^+$
58	100	100	9.1 ± 0.1	$NH_2C(CH_3)_2^+$
45	4	3		$HOCO^+$
42	42	60	11.8 ± 0.1[a]	$C_3H_6^+$
41	19	21		$C_3H_5^+$
40	5	0		$C_3H_4^+$
39	6	4		$C_3H_3^+$
30	7	22	13.0[a]	$NH_2CH_2^+$
29	3	3		NH_2CH^+
28	20	2		$HCNH^+$
27	4	3		$C_2H_3^+$
18	16	28		NH_4^+
				H_2O^+[a]
15	8	2		CH_3^+

Mass spectra and appearance energies. Ion assignments of m/z peaks.
[a] See text.

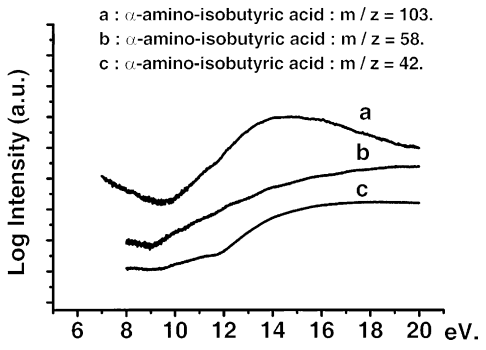

Fig. 8. Semi-log plots of photoion yield curves of α-aminoisobutyric acid: (a) $m/z = 103$; (b) $m/z = 58$; (c) $m/z = 42$.

same (unknown [33]) structure as that formed by ionization of propene, 14.81 eV if it has the (unknown) structure of the $m/z = 42$ fragment of ionized cyclopropane.

The yield curve of the $m/z = 42$ ion has a weak, slowly rising onset at 9.3 eV and a second, strongly rising onset at 11.8 eV (Fig. 8). Our experimental onset energy at 9.3 eV is incompatible with the $C_3H_6^+$ ion being one of the three cation structures mentioned above. The nature of the $C_3H_6^+$ ion at the initial onset at 9.3 eV remains unknown. Since the electron affinity of HOCO is 3.17 ± 0.13 [20], the 11.8 eV onset could be due to an ion pair reaction $NH_2C(CH_3)_2COOH \rightarrow NH_2C(CH_3)_2^+ + COOH^-$ followed by loss of NH_2 from the primary fragment ion.

3.5.2.4. $m/z = 39$–41. This P–COOH–NH_2 reaction is quite prevalent in α-amino acids, as is the P–COOH–NH_3 reaction which gives rise here to the $m/z = 41$ $C_3H_5^+$ ion whose structure is CH_3–CH=CH^+ [11]. The absence of a $m/z = 40$ ion in our photon impact mass spectrum and its presence in the 70 eV electron impact spectrum, coupled with the appearance of an ion $m/z = 39$ in both spectra, suggests that $m/z = 40$ is $C_3H_4^+$ and $m/z = 39$ is $C_3H_3^+$, and that the loss of a single hydrogen atom from $C_3H_5^+$ requires more energy than the loss of H_2. Alternative, but less probable, assignments are CH_2CN^+ for $m/z = 40$ and $HCCN^+$ for $m/z = 39$. The study of deuterium isotopologues would help clarify these assignments.

3.5.2.5. $m/z = 28$–30. The $m/z = 30$ fragment ion, whose appearance energy is in the 13 eV region, is assigned to $NH_2CH_2^+$, the formation of which requires hydrogen migration [11]. The $m/z = 29$ ion is considered to be NH_2CH^+, while the $m/z = 28$ ion, weak in our photon impact spectrum but strong in the electron impact spectrum, is assigned to $HCNH^+$. The contrasting relative intensities of the three ions $m/z = 30$, 29 and 28 in both mass spectra suggest that $m/z = 29$ and 28 are successive decomposition products of the $m/z = 30$ ion ($NH_2CH_2^+ \rightarrow NH_2CH^+ \rightarrow HCNH^+$), the fragmentation being more advanced with the higher energy deposition in the electron impact case.

3.5.2.6. Other fragment ions formed by dissociative ionization of α-aminoisobutyric acid. The fragment ion $m/z = 27$ could be either HCN^+ or $C_2H_3^+$. The relative intensity of this ion, with respect to possible precursors of HCN^+ (Table 4) inclines us to the $C_2H_3^+$ assignment, as in the case of α-alanine. The assignment of ions $m/z = 18$ and $m/z = 15$ to NH_4^+ and CH_3^+, respectively, is straightforward. The presence of a $m/z = 17$ peak in the mass spectrum and an increase in the $m/z = 18$ signal intensity at 12.6 eV indicates that a water impurity also contributes to the $m/z = 18$ mass spectral peak. We estimate its maximum contribution to be 12%, which enables us to determine a 10% minimum value for the branching ratio of NH_4^+ formation at 20 eV.

Finally, we remark that, judging from relative ion yields and fragment appearance energies, α-aminoisobutyric acid appears to be relatively more stable under 20 eV photons than glycine and the alanines. This is possibly related to the added conjugation introduced by the pseudo-π properties of the two methyl groups and it may contribute to the dominance of α-aminoisobutyric acid among the amino acids found in meteorites [2,3].

3.6. α-valine $NH_2(CH_3)_2(CH)_2COOH$ (elemental composition: $C_5H_{11}NO_2$)

The α-valine amino acid is proteinaceous. It can be derived from α-alanine by substituting two of its methyl hydrogens by methyl groups (Fig. 1). It has been observed in meteorites and micrometeorites [2,3]. Just as for other α-amino acids, it is capable in existing as many different conformers. The 70 eV electron impact mass spectrum data of α-valine published by Junk and Svec [11], given in the second column of Table 5, differs in some respects from that in the NIST compilation [20]. In particular it contains a strong peak at $m/z = 28$, strangely absent in the NIST spectrum, and the important $m/z = 74$ peak has a much greater intensity than in the NIST mass spectrum.

As can be seen from Table 5, there is good agreement between our 20 eV photon impact mass spectrum of α-valine (Fig. 2) and the electron impact mass spectrum of Junk and Svec [11]. Differences in relative peak intensities are considered to reflect different energy depositions in the two cases. One minor difference, however, between the two spectra is the presence of a considerable water impurity in our spectrum, which we estimate to contribute to at least 90% of the intensity of the $m/z = 18$ peak. We note the observation in our photon impact spectrum of a $m/z = 28$ peak which has a relative intensity similar to that of the electron impact spectrum of Junk and Svec (Table 5). Although we did not

Table 5
α-Valine: $NH_2(CH_3)_2(CH)_2COOH$

m/z	Electron impact 70 eV [11] relative intensity	Photon impact 20 eV relative intensity	Photon impact AE/eV	Ion
117	0.1	1	8.9[a]	$NH_2(CH_3)_2(CH)_2COOH^+$
75	16	12		$NH_2CH_2COOH^+$
74	34	45		$NH_2CHCOOH^+$
72	100	100		$NH_2(CH_3)_2(CH)_2^+$
57	29	60		$NHCHCOH^+$
56	11	Present but unresolved		$(CH_3)_2(CH)_2^+$
55	30	64		$C_4H_7^+$
46	5	13		NH_2CHOH^+
45	3	6		$HOCO^+$
43	7	13		$(CH_3)_2CH^+$
42	4	Unresolved		$C_3H_6^+$
41	8	9		$C_3H_5^+$
39	8	3		$C_3H_3^+$
30	12	19		$NH_2CH_2^+$
29	21	36		NH_2CH^{+a}
28	31	36		$HCNH^+$
27	9	6		$C_2H_3^{+a}$
18	4	[a]		[a]

Mass spectra and appearance energies. Ion assignments of m/z peaks.
[a] See text.

measure the appearance energy of the $m/z = 28$ ion, our results concerning the corresponding peak in the other α-amino acids studied make it most probable that it can be assigned to the $HCNH^+$ ion. This is supported by the α-valine-d_3 electron impact spectrum [11], which exhibits an equivalently intense peak at $m/z = 29$, as would be expected from a $HCND^+$ ion formed from a $ND_2(CH_3)_2(CH)_2COOD$ species. The absence of the $m/z = 28$ peak in the NIST spectrum must be an artefact of measurement or of reporting the results.

3.6.1. The parent ion $NH_2(CH_3)_2(CH)_2COOH^+$: $m/z = 117$

Our measurement of the IE of α-valine from the weak parent ion yield curve is not conclusive. There is a weak onset beginning at about 8.9 eV and a large increase in intensity beginning at 10.5 eV (Fig. 9). The only photoelectron spectrum of α-valine reported in the literature is by Klasinc [51] who gives IE(vert) = 9.68 eV and IE(ad) = 8.71 eV. The latter value is not very different from the weak onset at 8.9 eV observed in our PIMS study.

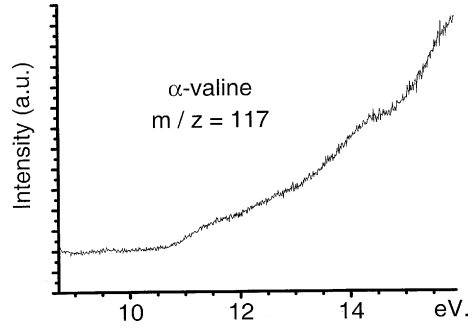

Fig. 9. Photoion yield curve of α-valine: $m/z = 117$.

3.6.2. Fragment ions of α-valine

The assignments of the fragment ions are given in Table 5. In very many cases they were confirmed by data from the α-valine-d_3 ($ND_2(CH_3)_2(CH)_2COOD$) electron impact spectrum [11]. Their ion yield curves were not measured.

3.6.2.1. $m/z = 75$. The $m/z = 75$ ion, which would be formed by loss of the dimethyl methylene group $C(CH_3)_2$, has a corresponding peak at $m/z = 78$, of the correct intensity, in the α-valine-d_3 mass spectrum [11]. However, its structure is unlikely to be that of glycine, $NH_2CH_2COOH^+$, and we concur with Junk and Svec [11], who assign it to the $H_2N{=}CHC{\cdot}(OH)_2^+$ ion, which is much more stable than the glycine ion [26,27]. The $m/z = 78$ ion in the α-valine-d_3 mass spectrum is consistent with a $D_2N{=}CHC{\cdot}OHOD^+$ structure.

3.6.2.2. $m/z = 74$. The important $m/z = 74$ ion, assigned to $NH_2CHCOOH^+$, is of undefined structure, but probably different from that of the $m/z = 74$ photoion formed in α-alanine (Table 2). It has a corresponding peak at $m/z = 77$ in the electron impact mass spectrum of α-valine-d_3 [11] and which has the same relative intensity (34%) as that of $m/z = 74$ in the α-valine mass spectrum (Table 5). This fragment ion is formed by loss of a $(CH_3)_2CH$ (isopropyl) radical. The corresponding charge switch reaction, leading to formation of the $(CH_3)_2CH^+$ ion ($m/z = 43$) also occurs, as is discussed

below. Since the isopropyl radical has an IE = 7.37 eV [20], the relative intensities of the $m/z = 74$ and $m/z = 43$ peaks indicate, from the SAH rule [55–57], that the IE of this form of $NH_2CHCOOH$ is probably closer to 7 eV.

3.6.2.3. $m/z = 72$ and 57. Assignments of the many other ions were also confirmed by peaks of correct intensity in the α-valine-d_3 mass spectrum (m/z values in parentheses). The most intense ion peak, at $m/z = 72$ (74), is assigned to $NH_2(CH_3)_2(CH)_2^+$, formed by loss of COOH following simple rupture of the C–C bond linking the carboxyl group to the α-carbon of α-valine. The $m/z = 57$ (58, 59) peak, which is assigned to $HN{=}CHC{\cdot}OH^+$ [11], is probably a product of dissociation of the $m/z = 75$ ion, $H_2N{=}CHC{\cdot}(OH)_2^+ \rightarrow HN{=}CHC{\cdot}OH^+ + H_2O$. The absence of a $m/z = 57$ peak in the glycine-h_5 mass spectrum is consistent with the interpretation that the $m/z = 75$ ion in the α-valine spectrum does not have the glycine structure.

3.6.2.4. $m/z = 56$ and 55. The $m/z = 56$ ion, present but insufficiently resolved in the photon impact spectrum is assigned to the $CH_3)_2(CH)_2^+$ ion, formed by loss of COOH and NH_2 from α-valine. If no hydrogen migration were involved, one would expect to find a $m/z = 56$ peak of similar intensity in the α-valine-d_3 spectrum. However the relative intensities of the peaks $m/z = 56$, 57, 58 in this spectrum [11] point to some hydrogen (deuterium) migration having occurred from the amino and carbonyl groups.

The important $m/z = 55$ species is assigned to $C_4H_7^+$, whose structure is suggested to be $CH_3CH_2CH{=}CH^+$ [11] formed by successive loss of COOH and NH_3. This apparently occurs without significant hydrogen migration since a peak of satisfactory intensity is found at $m/z = 55$ in the α-valine-d_3 mass spectrum.

3.6.2.5. $m/z = 39$–46. The $m/z = 46$ ion is probably NH_2CHOH^+, since an ion of corresponding intensity is observed at $m/z = 49$ in the d_3 mass spectrum. The alternative assignment, to $HCOOH^+$, is not supported by the α-valine-d_3 data.

The $m/z = 45$ peak assignment to the $HOCO^+$ ion is confirmed by the $m/z = 46$ peak in the α-valine-d_3 mass spectrum. Like the principal fragment ion $m/z = 72$, it is formed by simple rupture of the appropriate C–C bond. The relative intensities of the $m/z = 72$ and 45 peaks indicate that the ionization energy of the $NH_2(CH_3)_2(CH)_2$ moiety is less than that of the HOCO radical (8.06 ± 0.03 eV [34]). Although the IE of $NH_2(CH_3)_2(CH)_2$ has not been reported, it is very probable that it is in the 5–6 eV range as judged from the ionization energies [20] of the amino species formed in the analogous simple rupture reactions of the other α-amino acids studied: IE(NH_2CH_2) = 6.1 eV (formed in glycine); IE (NH_2CHCH_3) = 5.7 eV (formed in α-alanine); IE($NH_2C(CH_3)_2$) = 5.4 eV (formed in α-aminoisobutyric acid).

We next consider the set of fragment ions $m/z = 43$, 42, 41 and 39. These are all assigned as hydrocarbon ions (Table 5) and the assignments are supported by the observation of ions, having satisfactory peak intensities, at unchanged masses in the α-valine-d_3 mass spectrum [11], which shows that the amine and carboxyl group hydrogens are not involved in the formation of these fragments.

3.6.2.6. $m/z = 27$–30. The $m/z = 30$ ion is assigned to $NH_2CH_2^+$, consistent with the $m/z = 32$ ion observed in the α-valine-d_3 mass spectrum. The mass spectrum of this isotopologue was not of use for obtaining definitive assignments of the $m/z = 29$ and $m/z = 27$ peaks. Further studies on total or partially deuterated α-valine species are required for this purpose. The assignment to $HCNH^+$ of the intense peak at $m/z = 28$ was confirmed by the $m/z = 29$ peak in the α-valine-d_3 mass spectrum, as mentioned above.

3.6.2.7. $m/z = 18$ and 15. The importance of the water impurity in our photon mass spectrum prevented us from determining the true intensity of the NH_4^+ ion whose peak is at $m/z = 18$. That this peak in the electron impact spectrum is indeed due to the ammonium radical ion is confirmed by the presence of peaks at $m/z = 19$, 20 and 21 in the α-valine-d_3 mass spectrum, which indicates also that considerable hydrogen migration is involved in forming the NH_4^+ ion, including that of the hydrogen atom of the carboxyl group. Although α-valine contains two methyl groups, we did not observe a CH_3^+ peak at $m/z = 15$ in our 20 eV photon impact mass spectrum. This ion does appear very weakly (2% of the main peak) in the 70 eV electron impact mass spectrum but is much stronger in the electron impact spectra of other methyl-bearing species, α-alanine (5.3%) and α-aminoisobutyric acid (7.6%), where the effects of pseudo-π hyperconjugation appear to be less important.

4. Conclusion

Our PIMS study of five amino acids in the 6–22 eV photon energy range has provided new information on the ionization energies of these species and the nature and appearance energies of their dissociative ionization products. The assignment of the m/z peaks in the photon impact mass spectra, and analyses of fragment ion formation pathways, have been considerably assisted by data published by Junk and Svec [11] on the electron impact mass spectra of -d_3 isotopologues of three of these amino acids, as well as our own studies on photon excited glycine-d_5. Similar studies on deuterated

isotopologues of the β-alanine and α-aminoisobutyric acid would be useful for verifying and extending our proposed assignments and analyses in the case of these two non-proteinacous amino acids. Conspicuous among the dissociative photoionization reactions observed were those involving loss of COOH, COOH + NH_2 and COOH + NH_3, as previously found in electron impact studies on amino acids. Among our interesting observations that require further investigation are those involving formation of the astrophysically important $HCNH^+$ ion, which we suggest has a low energy formation channel different from that of a high energy channel in at least three of the five amino acids studied. In particular, ion-pair formation processes may be involved in initial stages of the low energy channel, as well as in the formation processes of other fragment ions in these five amino acids. A comparison between the results for the two forms of alanine, alpha and beta, shows that there is no isomeric conversion between their cations on VUV excitation up to 20 eV. Concerning the astrophysical implications of our study, described in more detail elsewhere [17], we note that the five amino acids would be easily photodissociated in HI regions of the interstellar medium since they exhibit fragmentation appearance energies well below 13.6 eV. Thus their observation in the interstellar medium calls for study of regions of radiation protection (dark clouds) or regions where amino acid production successfully outweighs destruction. This is confirmed by the very recent radioastronomical observation of glycine is in hot molecular core regions, where the visual extinction is very large, thus providing radiation protection [5]. The existence of amino acids in meteorites and micrometeorites also implies that their formation and survival occurs in conditions of efficient VUV radiation shielding.

Acknowledgements

Support from the CNRS Groupe de Recherche "GDR Exobiologie" and from the CNES convention with INSU is gratefully acknowledged.

References

[1] A. Brack (Ed.), The Molecular Origins of Life, Cambridge University Press, Cambridge, UK, 1998.
[2] J.R. Cronin in Ref. [1], p. 119.
[3] M. Maurette in Ref. [1], p. 147.
[4] L.E. Snyder, Origins Life Evol. Biosphere 27 (1997) 115.
[5] Y.-J. Kuan, S.B. Charnley, H.-C. Huang, W.-L. Tseng, Z. Kisiel, Astrophys. J. 593 (2003) 848.
[6] R. Briggs, G. Ertem, J.P. Ferris, J.M. Greenberg, P.J. McCain, C.X. Mendoza-Gomez, W. Schutte, Origins Life Evol. Biosphere 22 (1992) 287.
[7] K. Kobayashi, T. Kasamatsu, T. Kaneko, J. Koike, T. Oshima, T. Yamamato, H. Yanagawa, Adv. Space Res. 16 (1995) 21.
[8] R.S. Berry, S. Leach, Adv. Electron. Electron. Phys. 57 (1981) 1.
[9] J. Rak, P. Skurski, J. Simons, M. Gutowski, J. Am. Chem. Soc. 123 (2001) 11695.
[10] R.A. Jockusch, A.S. Lemoff, E.R. Williams, J. Am. Chem. Soc. 123 (2001) 12255.
[11] G. Junk, H. Svec, J. Am. Chem. Soc. 85 (1963) 839.
[12] T. Inagaki, Biopolymers 12 (1973) 1353.
[13] L. Serrano-Andes, M.P. Fülscher, J. Am. Chem. Soc. 118 (1996) 12200, and references therein.
[14] C. Chyba, C. Sagan, Nature 355 (1992) 125.
[15] M. Schwell, F. Dulieu, H.-W. Jochims, J.-L. Chotin, H. Baumgärtel, S. Leach, in: L.M. Celnikier, J. Trôn Than Vôn (Eds.), Proc. 12e Rencontres de Blois: "Frontiers of Life", 2000, The Gioi Publishers, Vietnam, 2002, p. 53.
[16] M. Schwell, F. Dulieu, S. Leach, Proc. First European Workshop on Exo-/Astro-Biology ESA SP-496, 2001, p. 133;
M. Schwell, F. Dulieu, S. Leach, Astrobiology 1 (2001) 210.
[17] S. Leach, in preparation.
[18] M. Schwell, F. Dulieu, C. Gée, H.-W. Jochims, J.-L. Chotin, H. Baumgärtel, S. Leach, Chem. Phys. 260 (2000) 261.
[19] CRC Spectrochemical Atlas: Registry of Mass Spectral Data, E. Stenhagen, S. Abramson, F.W. McLafferty, Wiley, NY, 1974.
[20] Data from National Institute of Standards and Technology, Standard Reference Database 69 – February 2000 Release: Nist Chemistry WebBook, http://webbook.nist.gov.
[21] P.H. Cannington, N.S. Ham, J. Electron Spectrosc. Rel. Phenom. 32 (1983) 139.
[22] T.P. Debies, J.W. Rabalais, J. Electron Spectrosc. Rel. Phenom. 3 (1974) 315.
[23] K. Iijima, K. Tanaka, S. Onuma, J. Mol. Struct. 246 (1991) 257.
[24] P.D. Godfrey, R.D. Brown, J. Am. Chem. Soc. 117 (1995) 2019.
[25] S.J. McGlone, P.S. Elmes, R.D. Brown, P.D. Godfrey, J. Mol. Struct. 485/486 (1999) 225.
[26] D. Yu, A. Rauk, D.A. Armstrong, J. Am. Chem. Soc. 117 (1995) 1789.
[27] F.G. Bordwell, X.-M. Zhang, M.S. Alnajjar, J. Am. Chem. Soc. 114 (1992) 7623.
[28] H.-G. Viehe, Z. Janousek, R. Merényi, L. Stella, Acc. Chem. Res. 18 (1985) 148.
[29] S. Simon, M. Sodupe, J. Bertran, J. Phys. Chem. A 106 (2002) 5697.
[30] L. Rodriguez-Santiago, M. Sodupe, A. Oliva, J. Bertran, J. Phys. Chem. A 104 (2000) 1256.
[31] H. Svec, G. Junk, J. Am. Chem. Soc. 89 (1967) 790.
[32] V.I. Saretskii, V.L. Sadovskaya, N.S. Wulfson, V.F. Sizoy, V.G. Merimson, Org. Mass Spectrom. 5 (1971) 1179.
[33] S.G. Lias, J.E. Bartmess, J.F. Libman, J.L. Holmes, R.D. Levin, W.G. Mallard, J. Phys. Chem. Ref. Data 17 (Suppl.No1) (1988).
[34] B. Ruscic, M. Litorja, Chem. Phys. Lett. 316 (2000) 45.
[35] B. Ruscic, M. Schwarz, J. Berkowitz, J. Chem. Phys. 91 (1989) 6780.
[36] E. Uggerud, H. Schwarz, J. Am. Chem. Soc. 107 (1985) 5046.
[37] D.J. DeFrees, A.D. McLean, J. Am. Chem. Soc. 107 (1985) 4350.
[38] P.C. Burgers, J.K. Terlouw, T. Weiske, H. Schwarz, Chem. Phys. Lett. 132 (1986) 69.
[39] J. Semaniak, B.F. Minaev, A.M. Derkatch, F. Hellberg, A. Neau, S. Rosén, R. Thomas, M. Larsson, H. Danared, A. Paál, M. af Ugglas, Astrophys. J. Suppl. Ser. 135 (2001) 275.
[40] Å.M.L. Øiestad, E. Uggerud, Int. J. Mass Spectrom. Ion Proc. 167/168 (1997) 117.
[41] P.C. Burgers, J.L. Holmes, J.K. Terlouw, J. Am. Chem. Soc. 106 (1984) 2762.
[42] P. Schilke, C.M. Walmsley, T.J. Millar, C. Henkel, Astron. Astrophys. 247 (1991) 487.
[43] G.J. Molina-Cuberos, J.J. Lopez-Moreno, R. Rodrigo, L.M. Lara, K. O'Brien, Planet. Space Sci. 47 (1999) 1347.

[44] P. Thaddeus, M. Guélin, R.A. Linke, Astrophys. J. 246 (1981) L41.
[45] Y.C. Minh, M.K. Brewer, W.M. Irvine, P. Friberg, L.E.B. Johansson, Astron. Astrophys. 244 (1991) 470.
[46] J. Berkowitz, Photoabsorption, Photoionization and Photoelectron Spectroscopy, Academic Press, New York, 1979, p.111.
[47] J.H. Beynon, R.A. Saunders, A.E. Williams, The Mass Spectra of Organic Molecules, Elsevier, Amsterdam, 1968.
[48] A.G. Császár, J. Phys. Chem. 100 (1996) 3541.
[49] K. Iijima, B. Beagley, J. Mol. Struct. 248 (1991) 133.
[50] R. Kaschner, D. Hohl, J. Phys. Chem. A102 (1998) 5111.
[51] L. Klasinc, J. Electron Spectrosc. Rel. Phenom. 8 (1976) 161.
[52] R.A.J. O'Hair, S. Blanksby, M. Styles, J.H. Bowie, Int. J. Mass Spectrom. 182/183 (1999) 203.
[53] F. Turecek, F.H. Carpenter, M.J. Polce, C. Wesdemiotis, J. Am. Chem. Soc. 121 (1999) 7955.
[54] F. Turecek, F.H. Carpenter, J. Chem. Soc., Perkin Trans. 2 (1999) 2315.
[55] D.P. Stevenson, Discuss. Faraday Soc. 10 (1951) 35.
[56] H.E. Audier, Org. Mass Spectrom. 2 (1969) 283.
[57] A.G. Harrison, C.D. Finney, J.A. Sherk, Org. Mass Spectrom. 5 (1971) 1313.
[58] S.J. McGlone, P.D. Godfrey, J. Am. Chem. Soc. 117 (1995) 1043.
[59] J.L. Holmes, F.P. Lossing, P. Mayer, J. Am. Chem. Soc. 113 (1991) 9723.
[60] D. Yu, A. Rauk, D.A. Armstrong, J. Chem. Soc., Perkin Trans. (2) (1994) 2207.
[61] M.V. Muftakhov, Y.V. Vasil'ev, V.A. Mazunov, Rapid Commun. Mass Spectrom. 13 (1999) 1104.
[62] L.C. Lee, R.W. Carlson, D.L. Judge, Mol. Phys. 30 (1975) 1941.
[63] K. Demyk, E. Dartois, L. d'Hendecourt, M. Jourdain de Muizon, A.M. Heras, M. Breitfellner, Astron. Astrophys. 339 (1998) 553.
[64] M.H. Engel, S.A. Macke, Nature 389 (1997) 265.
[65] W.V. Stelle, R.D. Chirico, A.B. Cowell, S.E. Knipmeyer, A. Ngyen, J. Chem. Eng. Data 42 (1997) 1053.
[66] R. Flammang, M.T. Nguyen, G. Bouchoux, P. Gerbaux, Int. J. Mass Spectrom. 202 (2000) A8.